2001

Microbially Catalyzed Nitrate-Dependent Oxidation of Biogenic Solid-Phase Fe(II) Compounds

Karrie A. Weber
University of Nebraska-Lincoln, kweber@unl.edu

Flynn W. Picardal
Indiana University - Bloomington

Eric E. Roden
The University of Alabama, ERODEN@BIOLOGY.AS.UA.EDU

Published in *Environmental Science & Technology* 35:8 (2001), pp. 1644–1650; doi: 10.1021/es0016598

Published online March 20, 2001

Microbially Catalyzed Nitrate-Dependent Oxidation of Biogenic Solid-Phase Fe(II) Compounds

Karrie A. Weber,[1] Flynn W. Picardal,[2] and Eric E. Roden [1]

1. Department of Biological Sciences, The University of Alabama, Tuscaloosa, Alabama 35487-0206
2. Environmental Science Research Center, School of Public and Environmental Affairs, Indiana University, Bloomington, Indiana 47405

Corresponding author — E. Roden, eroden@biology.as.ua.edu

Abstract

The potential for microbially catalyzed NO_3^--dependent oxidation of solid-phase Fe(II) compounds was examined using a previously described autotrophic, denitrifying, Fe(II)-oxidizing enrichment culture. The following solid-phase Fe(II)-bearing minerals were considered: microbially reduced synthetic goethite, two different end products of microbially hydrous ferric oxide (HFO) reduction (biogenic Fe_3O_4 and biogenic $FeCO_3$), chemically precipitated $FeCO_3$, and two microbially reduced iron(III) oxide-rich subsoils. The microbially reduced goethite, subsoils, and chemically precipitated $FeCO_3$ were subject to rapid NO_3^--dependent Fe(II) oxidation. Significant oxidation of biogenic Fe_3O_4 was observed. Very little biogenic $FeCO_3$ was oxidized. No reduction of NO_3^- or oxidation of Fe(II) occurred in pasteurized cultures. The molar ratio of NO_3^- reduced to Fe(II) oxidized in cultures containing chemically precipitated $FeCO_3$, and one of the microbially reduced subsoils approximated the theoretical stoichiometry of 0.2:1. However, molar ratios obtained for oxidation of microbially reduced goethite, the other subsoil, and the HFO reduction end products did not agree with this theoretical value. These discrepancies may be related to heterotrophic NO_3^- reduction coupled to oxidation of dead Fe(III)-reducing bacterial biomass. Our findings demonstrate that microbally catalyzed NO_3^--dependent Fe(II) oxidation has the potential to significantly accelerate the oxidation of solid-phase Fe(II) compounds by oxidized N species. This process could have an important influence on the migration of contaminant metals and radionuclides in subsurface environments.

Introduction

Direct microbial catalysis is responsible for the majority of iron(III) oxide reduction occurring in anoxic nonsulfidogenic natural systems (*1*−*3*). Enzymatic reduction of iron(III) oxides yields both soluble Fe(II) and a variety of solid-phase Fe(II) [Fe(II)(s)] compounds including minerals such as $Fe_3(PO_4)_2$, $FeCO_3$, and Fe_3O_4 as well as unspecified amorphous Fe(II) phases, including Fe(II) sorbed to iron(III) oxide surfaces and other minerals (*2*, *4*−*7*).

Oxidation of Fe(II) produced by bacterial iron(III) oxide reduction may occur via several different abiotic and biotic pathways. In aerobic environments at circumneutral pH, the chemical oxidation of Fe(II) by O_2 is a rapid and potentially dominant process (*8*). However, recent studies indicate that microaerophilic Fe(II)-oxidizing bacteria may contribute significantly to Fe(II) oxidation at circumneutral pH (*9*−*12*). Oxidation of Fe(II) is not limited to aerobic environments. Several abiotic and biotic Fe(II) oxidation processes are operative under anaerobic conditions. Anoxic Fe(II) oxidation can occur through the activity of anaerobic phototrophic, purple, nonsulfur bacteria (*13*). Manganese(IV) abiotically oxidizes Fe(II) at circumneutral pH (*14*). It has also been suggested that Fe(II) may be oxidized by NO_3^- in anaerobic, sedimentary environments (*10*, *15*−*20*. Abiotic reduction of NO_3^- to NH_4^+ by Fe(II) at a circumneutral pH occurs at high temperatures (75 °C) (*21*) and in the presence of green rust (*22*). The presence of trace metals such as Cu^{2+} (*23*−*25*) or crystalline iron oxide (lepidocrocite and goethite) surfaces (*25*) accelerates low-temperature reduction of NO_3^- coupled to Fe(II) oxidation at pH values greater than 8.0. Postma (*17*) concluded that, at low pH ranges, Fe(III) precipitates formed during iron silicate dissolution may catalyze oxidation of Fe(II) by NO_3^-.

The relatively specialized conditions required (i.e., high temperature, pH, catalyst) for abiotic Fe(II) oxidation by NO_3^- suggests that these reactions, with the exception of iron(III) oxide surface catalysts, may not be prevalent in typical natural sedimentary environments (*26*). Recently, denitrifying microorganisms capable of coupling Fe(II) oxidation to NO_3^- reduction to N_2 at circumneutral pH, in some cases under strict autotrophic conditions, have been identified (*11, 27*). Such organisms have been detected in a variety of freshwater sediments (*28*) as well as sewage sludge systems (*29, 30*).

The occurrence of microbially catalyzed NO_3^--dependent Fe(II) oxidation in a variety of natural systems suggests that this reaction may play a significant role in coupling the redox cycles of N and Fe in sedimentary environments. As opposed to abiotic NO_3^--dependent Fe(II) oxidation reactions, this biotic process proceeds readily at relatively low temperatures and circumneutral pH and does not require specific catalysts. This process has important implications for both NO_3^- removal and the formation of reactive iron(III) oxides in subsurface sediments. The latter process could significantly affect the migration of contaminant metals and radionuclides whose behavior is strongly influenced by sorption reactions at iron(III) oxide surfaces (*31, 32*). The impact of NO_3^- on contaminant metal/radionuclide geochemistry may be particularly significant at U.S. Department of Energy sites where NO_3^- is often present at high concentrations (*33*) as a result of its use in nuclear fuels reprocessing. Although competition between NO_3^- and Fe(III)-reducing bacteria is likely to play a major role in the overall impact of NO_3^- on Fe/metal contaminant biogeochemistry (*34*), NO_3^--dependent Fe(II) oxidation may present an important secondary mechanism for retarding migration of metals [divalent cations with a high affinity for iron(III) oxides such as Zn^{2+}, Pb^{2+}, and Hg^{2+}] and radionuclides in subsurface environments, specifically in sedimentary environments where NO_3^- enters zones of contaminant metal mobilization associated with bacterial iron(III) oxide reduction.

Although the capacity for microbially catalyzed NO_3^--dependent oxidation of soluble Fe(II) is well-documented, it is currently unknown whether Fe(II)(s) compounds are subject to oxidation via this metabolism. This is an important consideration given that solid Fe(II) phases are the dominant

Table 1. Characterization of Solid-Phase Fe(II) Compounds

Fe(II) phase	$Fe(II)_{HCl}$/total Fe_{HCl}[a]	mineral phases present[b]	surface area (m^2/g)[c]	SD[d]
chemically precipitated $FeCO_3$	0.95	siderite	23.2	10.0
HC-70	1.0	quartz kaolinite goethite	28.7	1.2
CP-90	0.88	goethite quartz kaolinite	21.1	0.97
goethite	0.93	goethite siderite	32.3	2.7
biogenic Fe_3O_4	0.44	magnetite goethite (trace)	82.9	3.5
biogenic $FeCO_3$	0.94	siderite goethite (trace)	3.01	0.78

a. Determined by 0.5 N HCl extraction. **b.** Solid-phase Fe mineral phases identified by XRD analyses (Phillips XRG 3100, Cu line source). **c.** Surface area determined by BET N_2 adsorption (Micromeritics Model Gemini); values are averages of triplicate samples. **d.** SD, standard deviation.

end products of bacterial iron(III) oxide reduction in soils and sediments. In this study, we examined the potential for microbially catalyzed NO_3^--dependent oxidation of several Fe(II)(s) compounds, analogous to reduced phases abundant in anaerobic, nonsulfidogenic sedimentary environments. The primary objective was to investigate the rate and extent to which solid-phase end products of microbial iron(III) oxide reduction can be oxidized by this microbial process.

Materials and Methods

Biological NO_3^-- and NO_2^--Dependent Fe(II) Oxidation. The NO_3^--reducing, Fe(II)-oxidizing enrichment culture described by Straub et al. (*27*) was used to examine Fe(II)(s) oxidation coupled to NO_3^- reduction. Duplicate bottles of anaerobic, $NaHCO_3$-buffered (30 mM, pH 6.8) growth medium (*27*) were amended with various Fe(II)(s) compounds (see below). Initial concentrations of 0.5 M HCl-extractable Fe(II) in the cultures ranged from ca. 2 to 20 mmol L^{-1}. Very little aqueous Fe(II) was present in cultures amended with Fe(II)(s) compounds (≤0.24 mM). Approximately 55% of the Fe(II) remained soluble in cultures amended with 10 mM $FeSO_4 \cdot 7H_2O$; the remainder was associated with Fe(II)(s) carbonate and Fe(II)(s) phosphate precipitates. NO_3^--reducing Fe(II)-bearing mineral slurries were amended with NO_3^- from sterile stock solutions to achieve concentrations of approximately 2.5−6 mM.

Duplicate cultures were inoculated (10% v/v) with the lithotrophic, denitrifying Fe(II)-oxidizing enrichment culture grown as described by Straub et al. (*27*). Duplicate Fe(II)(s) mineral slurries amended with a pasteurized (80 °C, 10 min) inoculum served as killed controls. Cultures were incubated statically in the dark at 30 °C.

Samples collected were analyzed for Fe(II), total Fe, NO_3^-, and NO_2^- (see below). N_2O was not measured in this study. However, previous studies with the lithotrophic NO_3^--dependent Fe(II)-oxidizing enrichment culture have not observed the production of N_2O (*27*).

Chemical Oxidation of Fe(II) by NO_2^-. Chemical oxida tion of Fe(II)(s) compounds by NO_2^- was examined under conditions similar to those present in the biological Fe(II) oxidation experiments. NO_2^- was added from anaerobic, sterile stock solutions to Fe(II)(s) compounds to achieve a NO_2^-:Fe(II) ratio of approximately 1:4. This ratio provided sufficient Fe(II) to permit complete reduction of NO_2^- to N_2. Samples were collected and analyzed for NO_2^-, Fe(II), and total Fe as described below.

Preparation and Characterization of Solid-Phase Fe(II) Compounds. Microbially reduced synthetic goethite and two microbially reduced iron(III) oxide-rich subsoils (HC-70 and CP-90; *35*) were generated by *Shewanella algae* strain BrY (ca. 10^8 tryptic soy broth-grown cells mL^{-1}) in $NaHCO_3$-buffered medium [pH 6.8, N_2:CO_2 (80:20) atmosphere] containing 4.4 mM NH_4Cl, 0.44 mM KH_2PO_4, 30 mM lactate, and vitamin and trace mineral solutions as previously described (*36*). Biogenic $FeCO_3$ was produced via the reduction of synthetic amorphous hydrous ferric iron oxide (HFO) by *Shewanella putrefaciens* strain CN-32 in similar $NaHCO_3$-buffered medium. To produce biogenic Fe_3O_4, HFO was reduced by strain CN-32 in PIPES-buffered medium (10 mM, pH 6.8, 100% N_2 atmosphere).

Microbially reduced iron(III) oxides were pasteurized (80 °C for 10 min), collected by centrifugation under anaerobic conditions, and washed twice with anaerobic $NaHCO_3$ buffer (pH 6.8) with the exception of biogenic Fe_3O_4, which was washed with anaerobic PIPES buffer (pH 6.8). The reduced minerals were dispensed into sterile anaerobic serum bottles and pasteurized again. Reduced mineral transfers occurred in an anaerobic glovebag (Coy Products; N_2:H_2; 95:5) in order to prevent Fe(II) oxidation. Lactate concentrations in the concentrated microbially reduced iron(III) oxide stocks were less than 15 μM, as determined by ion chromatography (IonPac AS14 analytical column, Dionex DX-100 system, Dionex Corp., Sunnyvale, CA).

X-ray diffraction (XRD; described below) was used to identify major Fe phases present in microbially reduced Fe mineral stock slurries (Table 1). Minor Fe phases or unreduced HFO may not have been detected by XRD. The nature of the Fe(II)(s) present in microbially reduced goethite and subsoils is unknown. However, the Fe(II)(s) is most likely present as surface precipitates or sorbed to the iron(III) oxide surface (*37*). Siderite was identified by XRD as a major Fe(II) phase in biogenic $FeCO_3$ cultures. Wet chemical analyses indicated that ca. 60% of total Fe(II)(s) was associated with carbonates (*38*). The remaining Fe(II)(s) was likely present as amorphous iron(II) hydroxide and/or sorbed Fe(II). XRD analysis verified the presence of magnetite in biogenic Fe_3O_4, and most of the Fe(II)(s) was likely present in this phase. The slight disagreement between the observed (0.44) and the theoretical (0.66) ratio of Fe(II):Fe(III) in this material may be a result of surface precipitation or sorption of Fe(II) to residual oxide surfaces.

Chemically precipitated $FeCO_3$ (siderite) was prepared by combining 250 mM Na_2CO_3 and 250 mM $FeCl_2$ under anaerobic conditions. The precipitate was centrifuged under N_2 and washed three times with anaerobic, deionized H_2O. The precipitate was resuspended, dispensed into anaerobic sterile serum bottles, and pasteurized. Production of siderite was confirmed by XRD analysis. Approximately 70% of the Fe(II)(s) was recovered as solid-phase carbonate.

Surface Area Analyses. Triplicate samples of the Fe(II)-bearing minerals were collected and dried under a stream of N_2 for 48 h. Quantification of Fe(II) and total Fe by 0.5 M HCl extraction and ferrozine analysis (see below) before and after drying indicated that the drying process did not cause oxidation of the Fe(II)-bearing minerals. The surface area of the minerals was analyzed by multipoint BET N_2 adsorption (Micromeritics Model Gemini).

X-ray Diffraction. Samples of microbially reduced iron(III) oxide minerals and chemically precipitated $FeCO_3$ were smeared onto petrographic slides and dried inside an anaerobic chamber for 48 h. To prevent oxidation of reduced Fe minerals, slides were then coated with ethyl cellulose dissolved in amyl acetate (8% w:v). Slides were stored anaero-

bically until XRD analyses on a Phillips XRG 3100 X-ray diffractometer with a Cu-line source.

Chemical Analyses. Samples for NO_3^- and NO_2^- were filtered through a 0.2-μm nylon filter and exposed to O_2, which rapidly oxidized Fe(II) and thereby prevented further reduction of NO_2^- by Fe(II) (*39*). The filtered samples were centrifuged, and the supernatant was withdrawn for NO_3^- and NO_2^- analysis. NO_3^- was determined by ion chromatography (IonPac AS14 analytical column, Dionex DX-100 system, Dionex Corp., Sunnyvale, CA). NO_2^- was determined colorimetrically (*40*) with a detection limit of 0.01 μM.

The amount of Fe(II) and total Fe extractable by 0.5 M HCl was determined as previously described (*4*). The difference between total Fe and Fe(II) in 0.5 M HCl represents poorly crystalline Fe(III) formed by NO_3^--dependent Fe(II) oxidation. Crystalline iron(III) oxides [goethite and Fe(III) phases in subsoils] were not liberated by the 0.5 M HCl extraction. Because NO_2^- spontaneously oxidizes Fe(II) at an acidic pH, Fe(II) determined by 0.5 M HCl extraction would be inaccurate if high concentrations of NO_2^- were present. To avoid such artifactual Fe(II) loss, samples for analyses of Fe concentrations were also collected by centrifugation under anaerobic conditions. The supernatant was withdrawn, and 0.5 M HCl was added to the pellet. The pellet was resuspended in acid and allowed to extract overnight. Fe(II) and total Fe in the extract were then determined using ferrozine. Aqueous Fe(II) was determined by analyzing an aliquot of sample filtered through a 0.2-μm nylon filter with ferrozine. The concentrations of 0.5 M HCl-extractable Fe(II)(s) determined via pellet extractions together with aqueous Fe(II) measurements were summed to yield total Fe(II) concentrations. This method yielded results equal to the 0.5 M HCl-extractable Fe(II) content of whole culture samples (aqueous + solid phase). Fe(II)-bearing mineral slurries amended with NO_2^-- (chemical oxidation studies) and NO_3^--reducing cultures containing biogenic Fe_3O_4 and biogenic $FeCO_3$ were analyzed in this manner due to the substantial concentrations of NO_2^-.

Data Presentation. Data are presented in the form of a ratio of the amount of Fe(II) to the total amount of Fe liberated by 0.5 M HCl extraction [$Fe(II)_{HCl}$/total Fe_{HCl}]. This approach reduced data scatter resulting from difficulty in obtaining subsamples of uniform particle content from suspensions of aggregated solids. Systematic changes in the total Fe content of the HCl extracts were not observed, which verified that all of the Fe(III) formed during NO_3^--dependent Fe(II) oxidation was recovered by the 0.5 M HCl extraction.

Results

Microbially Catalyzed NO_3^--Dependent Fe(II) Oxidation. No significant NO_3^- reduction or Fe(II) oxidation was observed in pasteurized control cultures (Figures 1−3). In contrast, rapid NO_3^--dependent oxidation of the following Fe(II)(s) minerals was observed in cultures inoculated with the enrichment culture described by Straub et al. (*27*): chemically precipitated $FeCO_3$ (Figure 1B), HC-70 (Figure 2A), CP-90 (Figure 2B), and goethite (Figure 2C). The significant random data fluctuations observed in some of the control cultures (especially the microbially reduced goethite and CP-90 subsoil) resulted from difficulty in obtaining samples of uniform particle content from suspensions of highly aggregated solids. Aqueous Fe(II) concentrations did not increase in pasteurized cultures over the course of the experiment (data not shown); thus the microbially catalyzed Fe(II)(s) oxidation observed in these studies cannot simply be attributed to dissolution of Fe(II)-bearing solids. As observed by Straub et al. (*27*), Fe(II) was rapidly oxidized in cultures amended with $FeSO_4$ (Figure 1A). NO_2^- concentrations did not exceed 15 μM in the above

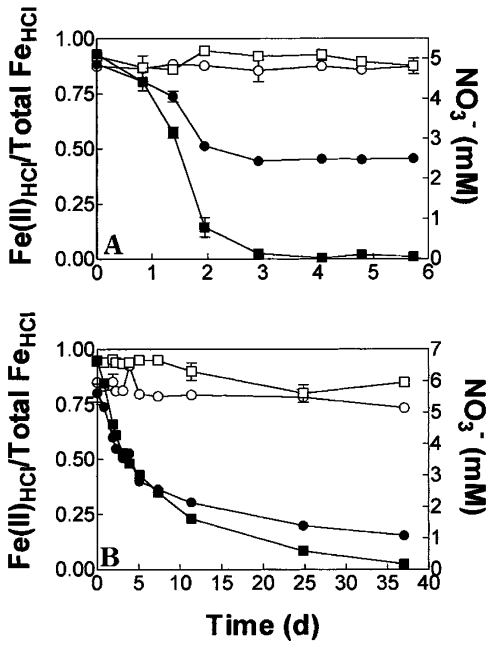

Figure 1. Biological NO_3^--dependent oxidation of (A) $FeSO_4$ [10 mM Fe(II)] and (B) chemically precipitated $FeCO_3$ [20 mmol of Fe(II) L^{-1}]. (■) $Fe(II)_{HCl}$/total Fe_{HCl} live culture; (□) $Fe(II)_{HCl}$/total Fe_{HCl} pasteurized culture; (●) NO_3^- live culture; (○) NO_3^- pasteurized culture. Error bars indicate ± range of duplicate cultures; bars not visible are smaller than the symbol.

cultures. Significant oxidation of biogenic Fe_3O_4 was observed (Figure 3A); a transient accumulation of NO_2^- was observed in these cultures. Although NO_3^- decreased and NO_2^- accumulated in live biogenic $FeCO_3$ cultures, very little of the Fe(II) present was oxidized (Figure 3B).

The rate and extent of Fe(II) oxidation varied substantially among the Fe(II)(s) minerals. Pseudo-first-order rate constants for Fe(II) oxidation were calculated by nonlinear least-squares regression fitting (Prism GraphPad) of Fe(II) vs time data to the following equation:

$$Fe(II)_t = [Fe(II)_{initial} - FE(II)_{final}] \exp(-kt) + FE(II)_{final} \quad (1)$$

Note that the quantity $[Fe(II)_{initial} - Fe(II)_{final}]$ represents the total amount of oxidizable Fe(II) at the start of the experiment and that $[Fe(II)_t - Fe(II)_{final}]$ represents the amount of oxidizable Fe(II) present at time t. Percent oxidation was calculated according to

$$\% \text{ oxidized} = [Fe(II)_{initial} - FE(II)_{final}] / Fe(II)_{initial} \times 100 \quad (2)$$

Goethite cultures exhibited the most rapid rate constant for Fe(II) oxidation (k = 1.08 d^{-1}) followed by the two subsoils (CP-90 and HC-70), $FeSO_4$, biogenic Fe_3O_4, chemically precipitated $FeCO_3$, and biogenic $FeCO_3$ (Table 2). Although goethite exhibited the fastest oxidation rate, the abiotic Fe(II) sources ($FeSO_4$ and chemically precipitated $FeCO_3$) exhibited the greatest extent of Fe(II) oxidation (97−99%), followed by HC-70 subsoil, goethite, biogenic Fe_3O_4, CP-90 subsoil, and biogenic $FeCO_3$ (Table 2). The most interesting difference in the rate and extent of oxidation was observed between the two forms of $FeCO_3$ (chemically precipitated $FeCO_3$ vs biogenic $FeCO_3$). Only 6% (ca. 1 mmol L^{-1}) of the biogenic $FeCO_3$ was oxidized with a first-order decay rate constant of 0.07 d^{-1}, whereas 97% (ca. 19 mmol L^{-1}) of the chemically precipitated $FeCO_3$ was oxidized with a first-order decay rate constant of 0.17 d^{-1}.

The molar ratio of NO_3^- reduced to Fe(II) oxidized in the $FeSO_4$ (0.26; r^2 = 0.996) and chemically precipitated $FeCO_3$

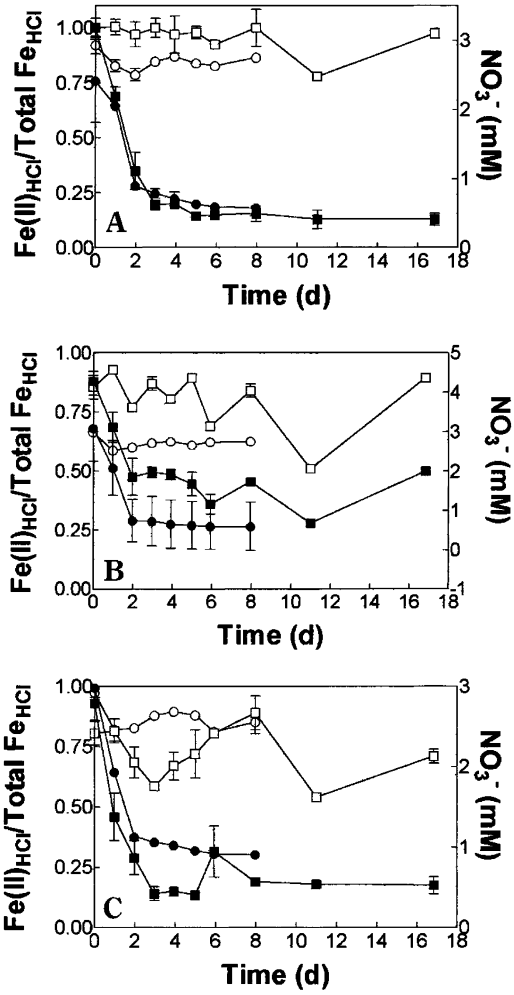

Figure 2. Biological NO_3^--dependent oxidation of (A) microbially reduced HC-70 subsoil [8 mmol of Fe(II) L^{-1}], (B) microbially reduced CP-90 subsoil [5 mmol of Fe(II) L^{-1}], and (C) microbially reduced goethite [2 mmol of Fe(II) L^{-1}]. Symbols are the same as in Figure 1. Error bars indicate ± range of duplicate cultures; bars not visible are smaller than the symbol.

(0.24; r^2 = 0.980) cultures agreed with the following equation and observations of Straub et al. (*27*):

$$10Fe^{2+} + 2NO_3^- + 24H_2O \rightarrow 10\,Fe(OH)_3 + N_2 + 18H^+ \quad (3)$$

The molar ratio of NO_3^- reduced to Fe(II) oxidized in the HC-70 subsoil cultures (0.26; r^2 = 0.859) also approximated the stoichiometry of eq 3. However, the molar ratio of NO_3^- consumed to Fe(II) oxidized in the CP-90 subsoil (0.83), goethite (1.21), and biogenic $FeCO_3$ (0.88) cultures did not agree with the theoretical stoichiometry. Whereas the molar ratios of NO_3^- consumed:Fe(II) oxidized in the chemically precipitated $FeCO_3$, $FeSO_4$, and HC-70 cultures remained constant throughout the course of Fe(II) oxidation, the ratio of NO_3^- to Fe(II) consumed during oxidation of biogenic Fe_3O_4 increased to 2.6 at 1.9 d, when NO_2^- concentrations were 0.3 mM, and then decreased to 0.5 by the end of the study. This observation is consistent with organotrophic reduction of NO_3^- to NO_2^- followed by organotrophic NO_2^- reduction and/or abiotic oxidation of Fe(II) by NO_2^- (see below).

Chemical Oxidation of Solid-Phase Fe(II)-Bearing Minerals by NO_2^-. To assess the potential significance of the abiotic oxidation of Fe(II)(s) by NO_2^- produced as an intermediate or end product of NO_3^- reduction, a series of chemical Fe(II) oxidation studies were conducted. For these experiments, pseudo-first-order rate constants were calculated according to eq 1 to allow for comparison with analogous rate constants for biological NO_3^--dependent Fe(II) oxidation. However, we recognize that the oxidation of Fe(II) by NO_2^- was not likely a first-order reaction at the concentrations of NO_2^- and Fe(II) used. NO_2^- oxidized Fe(II)(s) at an initially rapid rate (pseudo first-order rate constants of 2.9–9.1 d^{-1}) with the exception of biogenic and chemically precipitated $FeCO_3$, for which no oxidation of Fe(II) or reduction of NO_2^- was apparent after ~40 d (Table 3). Although an initially rapid rate of abiotic oxidation of Fe(II)(s) by NO_2^- was observed, the fraction of Fe(II) oxidized by NO_2^- (Table 3) was less than observed in live NO_3^--dependent Fe(II)(s) oxidation cultures (Table 2). The lack of complete Fe(II) oxidation was not due to exhaustion of NO_2^-, since substantial quantities (> 0.5 mM) remained at the end of each of the experiments. Molar ratios of NO_2^- reduced to Fe(II) oxidized for Fe(II)(s) containing HC-70 (0.33), goethite (0.36), and biogenic Fe_3O_4 (0.27) were in the range of the theoretical stoichiometries for reactions such as

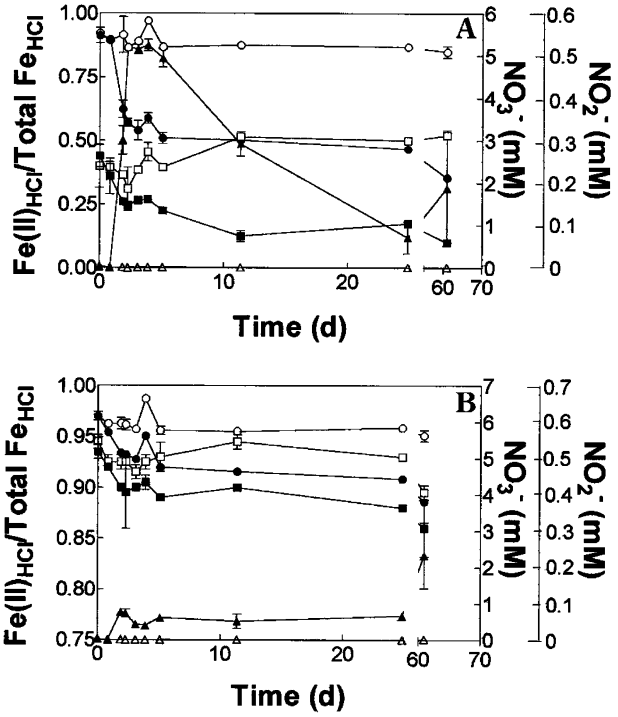

Figure 3. Biological NO_3^--dependent oxidation of (A) biogenic Fe_3O_4 [6 mmol of Fe(II) L^{-1}] and (B) biogenic $FeCO_3$ [20 mmol of (Fe(II) L^{-1}]. Symbols are the same as in Figure 1. (▲) NO_2^- live cultures; (Δ) NO_2^- pasteurized cultures. The *x*-axis is broken at 25 days and continues at 60 days in order to separate early data points. Error bars indicate ± range of duplicate cultures; bars not visible are smaller than the symbol.

$$6Fe^{2+} + 2NO_2^- + 14H_2O \rightarrow 6Fe(OH)_3 + N_2 + 10H^+ \quad (4)$$

$$4Fe^{2+} + 2NO_2^- + 9H_2O \rightarrow 4Fe(OH)_3 + N_2O + 6H^+ \quad (5)$$

The slurry amended with reduced CP-90 subsoil exhibited a molar ratio of NO_2^- reduced to Fe(II) oxidized (0.10) less than the predicted molar ratio.

Discussion

The lack of significant NO_2^- accumulation in NO_3^--reducing cultures containing $FeSO_4$, chemically precipitated $FeCO_3$, HC-70, CP-90, and goethite suggested that Fe(II) oxidation was coupled to direct reduction of NO_3^- to N_2. A kinetic model simulation of the $FeSO_4$ oxidation experiment was developed to assess the potential importance of NO_2^-,

Table 2. Biological NO_3^--Dependent Oxidation of Fe(II) Compounds

Fe(II) phase	Fe(II) (mmol L^{-1})	NO_3^- (mM)	time[a] (d)	% Fe(II) oxidized	molar ratio NO_3^- consumed:Fe(II) oxidized[b]	r^2	NO_3^--dependent Fe(II) oxidation $K^c(d^{-1})$	R^2
$FeSO_4$	9.1	4.9	6	99	0.26* ± 0.01	0.996	0.46[d]	0.995
chemically precipitated $FeCO_3$	20.3	5.6	37	97	0.24* ± 0.01	0.980	0.17 ± 0.01	0.986
HC-70	8.1	2.4	8	87	0.26* ± 0.03	0.859	0.63 ± 0.07	0.973
CP-90	5.2	2.4	11	49	0.83* ± 0.13	0.773	0.71 ± 0.11	0.855
goethite	2.0	3.0	8	80	1.21* ± 0.10	0.921	1.08 ± 0.23	0.916
biogenic Fe_3O_4	5.6	5.4	61	77	0.50* ± 0.10	0.746	0.29 ± 0.06	0.863
biogenic $FeCO_3$	18.7	6.1	61	6	0.88 ± 0.12	0.109	0.07 ± 0.03	0.573

a. Values represent the time when Fe(II) and NO_3^- concentrations are no longer significantly changed. **b.** Determined by linear least-squares regression analyses of NO_3^- vs total Fe(II) data for live cultures. Error terms represent the standard error of the slope. An asterisk (*) indicates statistical significance ($p < 0.05$). **c.** First-order rate constant (k) determined by nonlinear least-squares regression fitting (Prism GraphPad) of Fe(II) vs time to Equation 1 in the text. Error terms represent the standard error of *k*. **d.** Kinetics of this reaction did not follow a first-order rate equation. Half-life was determined by nonlinear least-squares regression fitting (Prism GraphPad) of Fe(II) vs time data to a sigmoidal variable slope equation and converting $t_{1/2}$ to *k* according to $k = \ln(2)/t_{1/2}$.

Table 3. Abiotic Oxidation of Fe(II) Compounds by NO_2^-

Fe(II)-bearing minerals	Fe(II) (mmol L^{-1})	NO_2^- (mM)	time[a] (d)	% Fe(II) oxidized	molar ratio NO_2^- consumed: Fe(II) oxidized[b]	r^2	NO_2^--dependent oxidation $k^c(d^{-1})$	R^2
$FeSO_4$	12.1	3.0	38	76[d]	0.38* ± 0.03	0.947	0.153	0.016
chemically precipitated $FeCO_3$	22.7	4.2	40[e]	0	na[f]	na	na	na
HC-70	7.9	2.2	7	32	0.19* ± 0.07	0.544	0.651 ± 0.23	0.720
CP-90	3.9	1.3	14	30	0.22 ± 0.18	0.178	0.229 ± 0.04	0.639
goethite	1.8	.5	2	25	0.11* ± 0.05	0.404	0.275 ± 0.26	0.500
biogenic Fe_3O_4	4.8	1.2	21	25	0.27* ± 0.11	0.519	2.92 ± 1.25	0.566
biogenic $FeCO_3$	18.63	3.7	40[e]	0	na	na	na	na

a. Values represent the time when Fe(II) and NO_2^- concentrations are no longer significantly changed. **b.** Determined by linear least-squares regression analyses of NO_2^- vs Fe(II) data. Error terms represent the standard error of the slope. An asterisk (*) indicates statistical significance ($p < 0.05$). **c.** First-order rate constant (*k*) determined by nonlinear least-squares regression (Prism GraphPad) fitting of Fe(II) vs time data to Equation 1 in the text. Error terms represent the standard error of *k*. **d.** Complete oxidation of $FeSO_4$ was not observed in this experiment due to exhaustion of NO_2^-. However, other experiments have shown complete abiotic oxidation of $FeSO_4$ by NO_2^-. **e.** Terminated at 40 days after no significant change. **f.** na = not applicable.

produced as an intermediate during NO_3^- reduction, as an abiotic oxidant during NO_3^--dependent Fe(II) oxidation (see Supporting Information). The model incorporated an experimentally determined rate constant for the reaction of $FeSO_4$ with NO_2^- derived from the abiotic oxidation experi ment reported in Table 3. Results of the simulation suggested that accumulation of NO_2^- far in excess of that observed in the cultures would have occurred if enzymatic NO_3^- reduction to NO_2^-, followed by abiotic oxidation of Fe(II) by NO_2^-, was the mechanism responsible for Fe(II) oxidation. It was not possible to conduct analogous simulations of the biogenic Fe(II)(s) oxidation experiments because of complexity introduced by the lack of complete abiotic Fe(II) oxidation by NO_2^-. However, the generally much lower degree of abiotic Fe(II)(s) oxidation by NO_2^- as compared to NO_3^--dependent microbial activity (mean = 32 ± 27%, $n = 6$) emphasizes the role of direct enzymatic reduction of NO_3^- to N_2 during Fe(II) oxidation. Particularly significant in this regard is the behavior of the chemically precipitated $FeCO_3$, which showed no reaction with NO_2^- but was rapidly oxidized enzymatically with little or no accumulation of NO_2^-.

Molar ratios of NO_3^- consumed:Fe(II) oxidized in experimental $FeCO_3$, $FeSO_4$, and HC-70 cultures approximated the theoretical stoichiometry of eq 3, suggesting that Fe(II)(s) was coupled to the reduction of NO_3^- to N_2. However, molar ratios in goethite, CP-90, biogenic $FeCO_3$, and biogenic Fe_3O_4 cultures exceeded the theoretical stoichiometry. The reason for this disagreement is unclear. Other studies of biological NO_3^--dependent Fe(II) oxidation have also observed molar ratios of NO_3^- consumed to Fe(II) oxidized in excess of theoretical values (*27, 30*). A purified, lithotrophic, NO_3^--reducing, Fe(II)-oxidizing culture (BrG2) consumed more NO_3^- than theoretically predicted (*27*). The authors speculated that some unidentified N species may have formed a stable complex with iron, a phenomenon that could also have taken place in our cultures. An alternative explanation is that organisms in the enrichment culture reduced NO_3^- organotrophically concurrent with Fe(II) oxidation, using dead cell biomass from the iron(III) oxide-reducing cultures as an energy source. NO_3^--reducing Fe(II)-oxidizing microorganisms have the ability to utilize a variety of organic substrates (*27*). The ability of the enrichment culture used in our experiments to oxidize lactate and other substrates coupled to NO_3^- reduction has been verified (K. Weber, unpublished data).

Heterotrophic NO_3^- reduction provides an explanation for the transient accumulation of NO_2^- in biogenic Fe_3O_4 cultures, given that the molar ratio of NO_3^- reduced to Fe(II) oxidized (0.5) exceeded theoretical predictions. This process probably occurred in other cultures (e.g., those containing microbially reduced goethite and CP-90 subsoil) but for unknown reasons did not lead to a significant accumulation of NO_2^-. The results of an attempt to observe biological NO_2^- reduction coupled to oxidation of biogeic Fe_3O_4 supports the conclusion that heterotrophic NO_3^- reduction was responsible for NO_2^- accumulation. In this experiment, virtually no difference was observed between the amount of Fe(II) oxidized by live and pasteurized cultures, while a significantly greater amount of NO_2^- was reduced in live cultures relative to pasteurized cultures (data not shown), i.e., additional reducing equivalents were obtained from sources other than Fe(II). However, it is important to note that the amount of biogenic Fe_3O_4 oxidized in NO_3^--reducing cultures cannot be accounted for alone by abiotic reaction with NO_2^- of organotrophic origin. The extent of abiotic Fe_3O_4 oxidation by

NO_2^- (25%; Table 3) was 3-fold less than that observed in live NO_3^--dependent Fe(II)-oxidizing cultures (77%; Table 2). Hence in the experiment shown in Figure 3A, a fraction of biogenic Fe_3O_4 was oxidized coupled to the biological reduction of NO_3^- as well as the abiotic reaction with NO_2^- produced via organotrophic NO_3^- reduction.

Fredrickson et al. (*7*) showed that in some cases biogenic Fe_3O_4 was not completely soluble in 0.5 M HCl but that 3 M HCl was able to effectively solublize the entire Fe content of such HFO reduction end products. Analysis of the biogenic Fe_3O_4 used in our experiments showed that 0.5 M HCl solublized 82% and 36% of the 3 M HCl-extractable Fe(II) and total Fe contents, respectively. The possibility exists that 0.5 M non-HCl-extractable Fe(II)(s) was more slowly and/or less extensively oxidized than 0.5 M HCl-extractable Fe(II)(s). If so, then the data reported here could represent an over estimation of rate and extent of overall Fe(II)(s) oxidized. However, the effect was likely minor since 0.5 M HCl recovered greater than 80% of the 3 M HCl-extractable Fe(II) content.

Very little of the Fe(II) in the biogenic $FeCO_3$ was oxidized. Heterotrophic NO_3^- reduction was thus probably responsible for much of the NO_2^- accumulation observed in these cultures. NO_2^- did not chemically oxidize biogenic $FeCO_3$ (Table 3). Hence, the 1 mmol Fe(II) L^{-1} that was oxidized in live biogenic $FeCO_3$ cultures was the result of biological catalysis. In contrast to the biogenic $FeCO_3$, 95% of the chemically precipitated $FeCO_3$ was oxidized at a rapid rate (Figure 1B, Table 2). The greater reactivity of chemically precipitated $FeCO_3$ to biological oxidation may be a result of the much greater (ca. 8-fold) surface area per unit mass (Table 2) available for microbial oxidation.

Environmental Significance. Most of the Fe(II)(s) phases examined were subject to rapid NO_3^--dependent oxidation in the presence of active microbial metabolism. In contrast, no significant NO_3^--dependent Fe(II) oxidation occurred in cultures containing heat-killed cells. Although a recent study demonstrated that Fe(II) associated with iron(III) oxide (goethite) surfaces was subject to abiotic oxidation by NO_3^- (half-life of NO_3^- for 10 g wet weight goethite was 1600 min; *25*). However, significant abiotic oxidation of Fe(II)(s) by NO_3^- did not occur under the culture conditions in this study. Although most of the Fe(II)(s) compounds used in this study were subject to significant chemical oxidation by NO_2^-, NO_3^--dependent Fe(II) oxidation was substantially more efficient than abiotic oxidation by NO_2^-. In addition, only minor concentrations of NO_2^- were formed during biological NO_3^--dependent Fe(II)(s) oxidation, which indicated that Fe(II)(s) oxidation was coupled directly to NO_3^- reduction to N_2. These findings indicate that microbial activity has the potential to vastly accelerate the coupling of N and Fe redox cycles in sedimentary environments.

Microbially catalyzed NO_3^--dependent Fe(II) oxidation could have a significant influence on the fate of NO_3^- in subsurface environments, particularly environments with a limited supply of organic carbon. Inverse correlations between NO_3^- and surface-bound Fe(II) in subsoil profiles have been observed (*15*, *18*, *19*). Although the authors have attributed this observation to the reduction of NO_3^- by Fe(II) (*15*, *18*, *19*), whether NO_3^- reduction was abiotically or biotically coupled to the oxidation of Fe(II) was not determined. A recent study concluded that microorganisms were not responsible for reduction of NO_3^- and oxidation of Fe(II) in these environments (*20*). However, this study examined heterotrophic NO_3^- reduction rates and quantified the abundance of aerobic heterotrophs; the potential for anaerobic NO_3^--dependent Fe(II) oxidation was not examined. The identification of NO_3^--dependent Fe(II) oxidizing microorganisms in a variety of environments (*11, 28*−*30*) suggests that these organisms could inhabit sediments investigated by Lind, Ernsten and colleagues. Biological NO_3^--dependent Fe(II)(s) oxidation could provide an explanation for chemical profiles of NO_3^- and Fe(II)(s) observed in these subsoil environments.

The formation of reactive iron(III) oxides, as a result of biological NO_3^--dependent Fe(II) oxidation, has the potential to exert a major influence on the aqueous geochemistry of anaerobic soils and sediments. The mobility of contaminant metals and radionuclides is influenced strongly by adsorption to reactive iron(III) oxide surfaces (*32*). Recent studies in our laboratory indicate that adsorption of Zn to biogenic iron(III) oxide surfaces produced by microbial NO_3^--dependent oxidation of $FeSO_4$ is comparable to adsorption of Zn to a relatively high surface area goethite produced by air oxidation of $FeCl_2$ (K. Weber, unpublished data). In addition to the possibility for metal/radionuclide sorption to reactive iron(III) oxide surfaces, the potential also exists for trapping of contaminant metals via coprecipitation with iron(III) oxides formed during NO_3^--dependent Fe(II) oxidation. Further studies examining the kinetics of NO_3^--dependent oxidation of microbially reduced iron(III) oxides and the reactivity of the resulting end products are required to understand the impact that this process may exert on the fate of contaminant metals and radionuclides in sedimentary environments.

Acknowledgments — Thanks to Dr. Kristina L. Straub for providing the NO_3^--dependent Fe(II)-oxidizing enrichment culture, Dr. Matilde Urrutia for assistance with surface area analyses, and Dr. D. Craig Cooper for XRD analyses. This research was supported by the Department of Energy, Natural and Accelerated Bioremediation Program, through Grant DE-FG02-97ER62482.

Supporting Information — A description of the development and results of the kinetic model simulation of the $FeSO_4$ oxidation experiment (4 pages) is presented following the **References.**

References

(1) Lovely, D. R. *Microbiol. Rev.* 1991, *55*, 259−287.

(2) Lovely, D. R. *Annu. Rev. Microbiol.* 1993, *47*, 263−290.

(3) Nealson, K. H.; Saffarini, D. A. *Annu. Rev. Microbiol.* 1994, *48*, 311−348.

(4) Roden, E. E.; Lovely, D. R. *Appl. Environ. Microbiol.* 1993, *59*, 734−742.

(5) Roden, E. E.; Wetzel, R. G. *Limnol. Oceanogr.* 1996, *41*, 1733−1748.

(6) Urrutia, M. M.; Roden, E. E.; Fredrickson, J. K.; Zachara, J. M. *Geomicrobiology* 1998, *15*, 269−291.

(7) Fredrickson, J. K.; Zachara, J. M.; Kennedy, D. W.; Dong, H.; Onstott, T. C.; Hinman, N. W.; Li, S. *Geochim. Cosmochim. Acta* 1999, *62*, 3239−3257.

(8) Stumm, W.; Morgan, J. J. *Aquatic Chemistry: Chemical Equilibria and Rates in Natural Waters*, 3rd Ed.; John Wiley & Sons: New York, 1996.

(9) Emerson, D.; Revsbech, N. P. *Appl. Environ. Microbiol.* 1994, *60*, 4032−4038.

(10) Emerson, D.; Moyer, C. L. *Appl. Environ. Microbiol.* 1997, *63*, 4784−4792.

(11) Benz, M.; Brune, A.; Schink, B. *Arch. Microbiol*. 1998, *169*, 159−165.

(12) Emerson, D.; Weiss, J. V.; Megonigal, J. P. *Appl. Environ. Microbiol.* 1999, *65*, 2758−2761.

(13) Widdel, F.; Schnell, S.; Heising, S.; Ehrenreich, A.; Assmus, B.; Schink, B. *Nature* 1993, *362*, 834−835.

(14) Postma, D. *Geochim. Cosmochim. Acta* 1985, *54*, 1023−1033.

(15) Lind, A. M. In *Denitrification in the Nitrogen Cycle*; Golterman, H. M., Ed.; Plenum: New York, 1983; pp 145−156.

(16) Verdegem, L.; Baert, L. *Pedologie* 1985, *36*, 39−54.

(17) Postma, D. *Geochim. Cosmochim. Acta* 1990, *54*, 903−908.

(18) Ernstsen, V.; Mørup, S. *Hyperfine Interact.* 1992, *70*, 1001−1004.

(19) Ernstsen, V. *Clays Clay. Miner.* 1996, *44*, 599−608.

(20) Ernstsen, V.; Binnerup, S. J.; Sørensen, J. *Geomicrobiology* 1998, *15*, 195−207.

(21) Petersen, H. J. S. *Acta Chem. Scand.* 1979, *33*, 795−796.

(22) Hansen, H. C. B.; Koch, C. B.; Nancke-Krogh, H.; Borggaard, O. K.; Sørensen. *Environ. Sci. Technol.* 1996, *30*, 2053−2056.

(23) Buresh, R. J.; Moraghan, J. T. *J. Environ. Qual.* 1976, *5*, 320−325.

(24) Van Hecke, K.; Van Cleemput, O.; Baert, L. *Environ. Pollut.* 1990, *63*, 261−274.

(25) Ottley, C. J.; Davison, W.; Edmunds, W. M. *Geochim. Cosmochim. Acta* 1997, *61*, 1819−1828.

(26) Langmuir, D. *Aqueous Environmental Geochemistry*; Prentrice-Hall: Englewood Cliffs, NJ, 1997.

(27) Straub, K. L.; Benz, M.; Schink, B.; Widdel, F. *Appl. Environ. Microbiol.* 1996, *62*, 1458−1460.

(28) Straub, K. L.; Buchholz-Cleven, B. E. E. *Appl. Environ. Microbiol.* 1998, *64*, 4846−4856.

(29) Nielsen, J. L.; Nielsen, P H. *Water Sci. Technol.* 1998, *37*, 403−406.

(30) Nielsen, J. L.; Nielsen, P H. *Environ. Sci. Technol.* 1998, *32*, 3556−3561.

(31) Davis, J. A.; Kent, D. B.; Rea, B. A.; Maest, A. S.; Garabedian, S. P. In *Metals in Groundwater*; Allen, H. E., Perdue, E. M., Brown, D. S., Eds.; Lewis Publishers: Boca Raton, FL, 1993; pp 223−273.

(32) Hering, J. G. In *Metal Speciation and Contamination of Soil*; Allen, E. A., Huang, C. P., Bailey, G. W., Bowers, A. R., eds.; Lewis Publishers: Boca Raton, FL, 1995; pp 59−86.

(33) Riley, R. G.; Zachara, J. M.; Wobber, F. J. U.S. Department of Energy Report DOE/ER-0547. 1992.

(34) Sorensen, J. *Geomicrobiology* 1987, 5, 401−421.

(35) Roden, E. E.; Zachara, J. M. *Environ. Sci. Technol.* 1996, *30*, 1618−1628.

(36) Lovely, D. R.; Phillips, E. J. P. *Appl. Environ. Microbiol.* 1988, *54*, 1472−1480.

(37) Roden, E. E.; Urrutia, M. M. *Environ. Sci. Technol.* 1999, *33*, 1847−1853.

(38) Roden, E. E.; Leonardo, M. R.; Ferris, F. G. Manuscript in preparation.

(39) Sørensen, J.; Thorling, L. *Geochim. Cosmochim. Acta* 1991, *55*, 1289−1294.

(40) Wetzel, R. G.; Likens, G. E. *Limnological Analyses*; Springer-Verlag: New York, 1991.

Supplementary Information – Kinetic modeling of nitrate-dependent oxidation of $FeSO_4$

The goal of the modeling exercise was to assess whether or not abiotic reaction of $FeSO_4$ with NO_2^- would be fast enough to prevent significant NO_2^- accumulation if enzymatic reduction of NO_3^- to NO_2^-, followed by abiotic reduction of NO_2^- to N_2, was the mechanism responsible for NO_3^--dependent Fe(II) oxidation. This coupled mechanism is illustrated by the following reaction scheme:

$$2Fe(II) + NO_3^- \rightarrow 2Fe(III) + NO_2^- \qquad \text{(enzymatic)} \qquad (1)$$

$$n\,Fe(II) + NO_2^- \rightarrow n\,Fe(III) + \text{reduced N} \qquad \text{(abiotic)} \qquad (2)$$

where n represents the ratio Fe(II) to NO_2^- consumption during the abiotic reaction between these two species (see below), and "reduced N" represents one or more N end-products with an oxidation state lower than +3.

The model simulates the time variation of NO_3^-, NO_2^-, and Fe(II) during NO_3^--dependent oxidation of $FeSO_4$ according to the above reaction scheme. The simulation is driven by the observed time course of NO_3^- consumption over time in the $FeSO_4$ cultures. The NO_3^- vs. time data (Fig. 1A in Weber et al., 2001; see also Suppl. Mat. Fig. 1C) data were fit by nonlinear least-squares regression to a sigmoidal function

$$C(t) = C_{min} + (C_{max} - C_{min})/(1 + 10\text{^}(\log t_{1/2} - t)) \qquad (3)$$

where C(t) is the NO_3^- concentration at time t; C_{min} is the minimum concentration of NO_3^-, observed at the end of the experiment; C_{max} is the maximum concentration of NO_3^-, present at the start of the experiment; and $t_{1/2}$ is time at which half of the total amount of NO_3^- consumed during the experiment has been utilized, i.e. the time at which $C(t) = 0.5(C_{max} - C_{min})$. This fitting function was not chosen on theoretical grounds, but rather was used because it provided

the most accurate empirical fit of the NO_3^- vs time data. Instantaneous rates of NO_3^- reduction were computed by evaluating the first derivative of equation 3 with respect to time:

$$R_{NO3}(t) = dC(t)/dt = (C_{max} - C_{min})/(1 + 10\text{^}(\log t_{1/2} - t))\text{^}2*10\text{^}(\log t_{1/2} - t)*\ln 10 \quad (4)$$

This rate term was incorporated into the following system of differential equations describing the rate of change of NO_3^-, NO_2^-, and Fe(II) concentration over time:

$$d[NO_3^-]/dt = -R_{NO3}(t) \quad (5)$$

$$d[NO_2^-]/dt = R_{NO3}(t) - (1/n)k[Fe(II)]^n[NO_2^-] \quad (6)$$

$$d[Fe(II)]/dt = -2R_{NO3}(t) - k[Fe(II)]^n[NO_2^-] \quad (7)$$

This set of equations assumes that enzymatic reduction of NO_3^- coupled to Fe(II) oxidation leads to production of NO_2^- according to a 1:2 ratio, and that consumption of NO_2^- occurs solely via abiotic reaction with Fe(II) according to a mass action rate law of order $(1+n)$ (*1*).

The rate constant for $FeSO_4$ oxidation by NO_2^- (k) was obtained from an experiment conducted in sterile growth medium. The composition of the medium was identical to that used for the biological NO_3^--dependent Fe(II) oxidation experiments. The rate constant was estimated by numerically integrating (using a fifth-order Runga-Kutta algorithm with truncation error control, obtained from ref. *2*) the following set of mass action expressions which describe the rates of Fe(II) and NO_2^- consumption during abiotic $FeSO_4$ oxidation by NO_2^- according to a $(1+n)^{th}$ order rate law:

$$d[Fe(II)]/dt = -k[Fe(II)]^n[NO_2^-] \quad (8)$$

$$d[NO_2^-]/dt = -(1/n)k[Fe(II)]^n[NO_2^-] \quad (9)$$

and varying the value of k in order to obtain an approximate best-fit to the observed Fe(II) and NO_2^- vs. time data (Suppl. Info., Fig. 1A). Initial Fe(II) and NO_2^- concentrations were set equal to the average values measured at the start of the abiotic oxidation experiment, and the value of n

was obtained from the slope of a scatter plot of the observed Fe(II) vs. NO_2^- concentrations during the experiment (Suppl. Info., Fig. 1B).

Using the values of *k* and *n* obtained from the abiotic oxidation experiment, the system of coupled equations 5-7 was integrated numerically over a six-day time period. Initial NO_3^-, NO_2^-, and Fe(II) concentrations were set equal to those measured at the start of the biotic NO_3^--dependent $FeSO_4$ oxidation experiment (ca. 5, 0, and 9 mM, respectively). The results of the simulations (Suppl. Info. Fig.1C) indicate that accumulation of NO_2^- in excess of 2 mM would have occurred if the mechanism described by equations 1 and 2 was responsible for NO_3^--dependent Fe(II) oxidation activity. In contrast, measured concentrations of NO_2^- in the $FeSO_4$ cultures never exceeded 0.015 mM. The simulation also predicted much slower consumption of Fe(II) over time than was observed in the experiment. These disparities lead to the conclusion that direct enzymatic reduction of NO_3^- to N_2 was responsible for $FeSO_4$ oxidation in the experiment shown in Fig. 1A in Weber et al., submitted.

Literature Cited

(1) Schnoor, J.L. *Environmental modeling*; John Wiley & Sons: New York, NY, 1996.

(2) Press, W.H.; Teukolsky, S.A.; Vetterling, W.T.; Flannery, B.P. *Numerical recipes in FORTRAN*; Cambridge University Press: Port Chester, NY, 1992, Vol. 1.

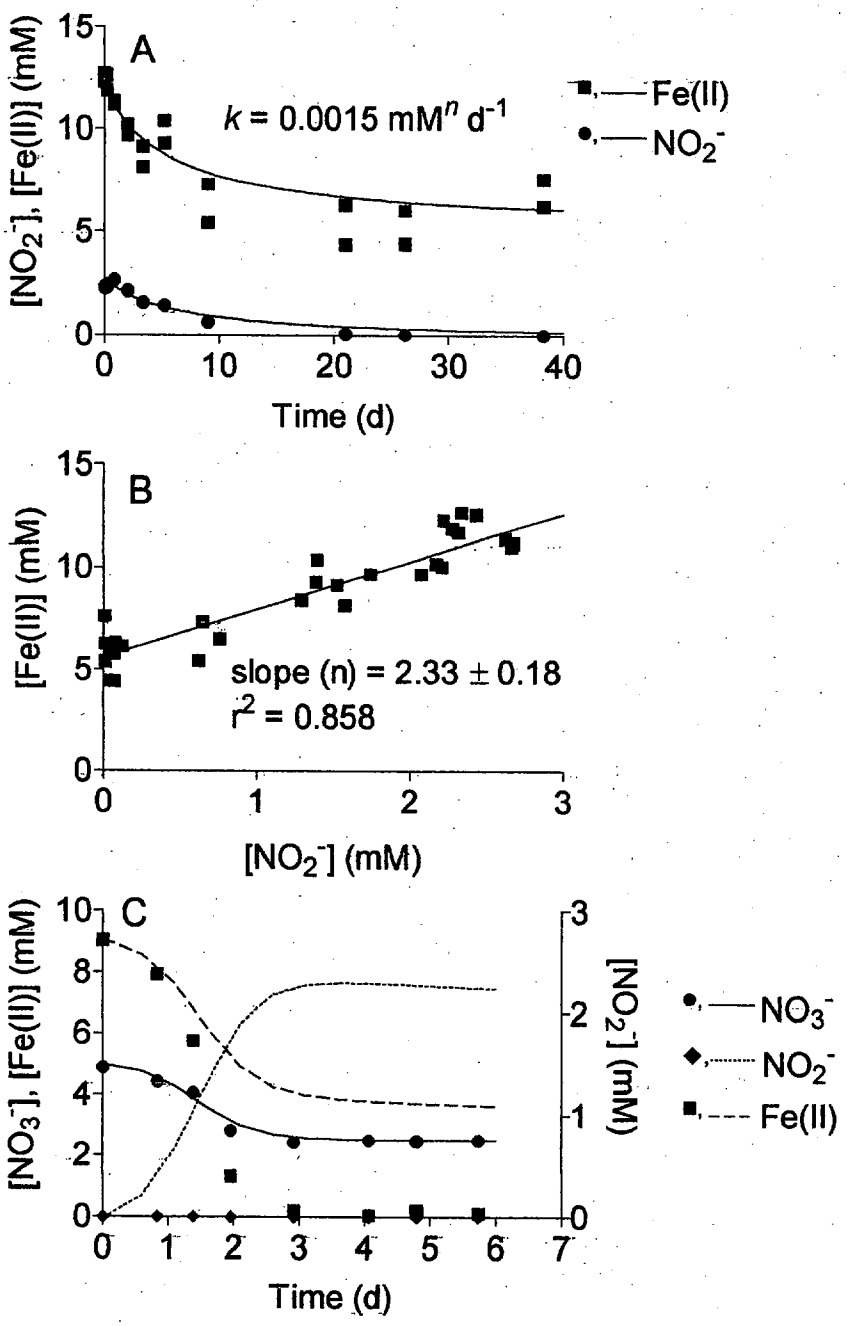

Suppl. Info. Fig. 1. Panel A: Abiotic oxidation of $FeSO_4$ by NO_2^- in sterile growth medium. Symbols represent measured concentrations in triplicate reactions systems; lines represent results of numerical integrations used to estimate the rate constant k (see text). Mean initial Fe(II) and NO_2^- concentrations were 12.1 and 2.75 mM, respectively. Panel B: [Fe(II)] vs. [NO_2^-] during abiotic oxidation of $FeSO_4$ by NO_2^-. Panel C: Results of simulation model. Symbols represent mean measured concentrations of Fe(II), NO_3^-, and NO_2^- in the biological $FeSO_4$ oxidation experiment (Fig. 1A in Weber et al. 2001).